

# Real-Time Surface Identification System for Variable Walking Speeds of Biped Robots

Aiwen Luo<sup>1</sup>, Member, IEEE, Sandip Bhattacharya<sup>2</sup>, Member, IEEE,  
Mitiko Miura-Mattausch<sup>3</sup>, Life Fellow, IEEE, Yicong Zhou<sup>4</sup>, Senior Member, IEEE,  
and Hans J. Mattausch<sup>5</sup>, Senior Member, IEEE

**Abstract**—Identifying the underlying surface at varying speeds during robotic locomotion is important for safe and efficient robot navigation. This work aims to enhance the perceptual abilities of biped robots by enabling the force sensor affixed beneath each foot to recognize multiple indoor surfaces while navigating at varying speeds. An accurate yet cost-efficient surface-identification system for the robot is proposed by combining a real-time multiobject support vector machine (SVM) with an efficient time-domain feature. In this context, four promising hand-crafted time-domain features are investigated, among which the root mean square (RMS) feature is proven to outperform the other three features. A mean average precision (mAP) of 95.99% and 98.16% in tenfold SVM cross-validation can be achieved by applying RMS at two different walking speeds, respectively. The high classification accuracy is achieved with high computing efficiency and thus enables system deployment on low-cost platforms, such as Arduino or Jetson Nano, which makes our approach suitable for a wide range of applications across varying walking speeds.

**Index Terms**—Biped robot, force sensor, real-time support vector machine (SVM), surface identification, variable walking speed.

## I. INTRODUCTION

INTELLIGENT service robots have been receiving significant attention over the last decade, driven by strong economic growth, increasing urbanization, and the health demands of an aging population around the world. Especially, the mobility impairment of the elderly leads to urgent support requirements with respect to home services and healthcare,

Manuscript received 6 June 2023; revised 8 July 2023 and 13 July 2023; accepted 23 July 2023. Date of publication 26 July 2023; date of current version 30 May 2024. This work was supported in part by the TAOYAKA Program for Creating a Flexible, Enduring, Peaceful Society at Hiroshima University; in part by the National Natural Science Foundation of China under Grant 62002134; in part by the Guangdong Basic and Applied Basic Research Foundation under Grant 2020A1515110645 and Grant 2023A1515010834; and in part by the Key Laboratory of New Semiconductors and Devices of Universities in Guangdong Province under Grant 2021KSY001. This manuscript was recommended for publication by H. Tomiyama. (Corresponding author: Aiwen Luo.)

Aiwen Luo is with the Department of Electronic Engineering, Jinan University, Guangzhou 510632, China, and also with the HiSIM Research Center, Hiroshima University, Higashihiroshima 739-8530, Japan (e-mail: faith.awluo@gmail.com).

Sandip Bhattacharya was with the HiSIM Research Center, Hiroshima University, Higashihiroshima 739-8530, Japan. He is now with the Department of Electronics and Communication Engineering, SR University, Warangal 506371, India (e-mail: 1983.sandip@gmail.com).

Mitiko Miura-Mattausch and Hans J. Mattausch are with the HiSIM Research Center, Hiroshima University, Higashihiroshima 739-8530, Japan (e-mail: hjm@hiroshima-u.ac.jp).

Yicong Zhou is with the Department of Computer and Information Science, University of Macau, Macau, China (e-mail: yicongzhou@um.edu.mo).

Digital Object Identifier 10.1109/LES.2023.3299114

1943-0671 © 2023 IEEE. Personal use is permitted, but republication/redistribution requires IEEE permission.

See <https://www.ieee.org/publications/rights/index.html> for more information.

Authorized licensed use limited to: Universidade de Macau. Downloaded on May 31, 2024 at 23:56:34 UTC from IEEE Xplore. Restrictions apply.

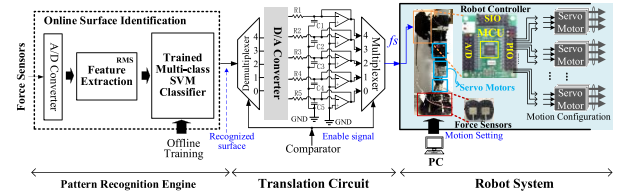


Fig. 1. Overall architecture of the proposed surface-identification system.

such as providing feeding support, mobility guidance, or rehabilitation therapy. Over the years, to support the predictive control of robotic locomotion on various ground surfaces, pattern recognition techniques, and intelligent control methods have been applied for surface classification in diverse robotic-locomotion options, such as wheeled [1], hexapod [2], quadruped [3], and biped robots [4], [5], [6]. A comparative study of different surface classification methods is reported in [6] based on multiple available sensors, including image, force, current, position, and inertial sensors. In most cases, multiple sensing modalities are combined for higher accuracy. Nevertheless, image sensors, Radar, and Lidar normally suffer from high computing complexity [12], so that more hardware resources and processing time are required. Surface identification can be implemented by different classifiers, such as decision trees (DTs) [4], random forests (RFs) [5],  $k$ -nearest-neighbor (kNN) [7], and artificial neural networks (ANNs) [8]. There is no common opinion on which classification model is better than others for robotic terrain perception. However, ANNs-based strategies normally achieve higher accuracy than other traditional classifiers, such as a support vector machine (SVM) at the cost of much higher resource consumption.

It is important to predict the properties of the underlying surface ahead of the robotic locomotion for safe and efficient navigation. Specifically, biped robots aim to reproduce human-like appearance and capabilities in different interesting topics and are expected to be able to traverse different ground surfaces with a highly dynamic balance on two feet. To provide a cost-effective, real-time surface identification system for resource-constrained biped robots operating at varying walking speeds, we proposed a sole-sensor-based solution as illustrated in Fig. 1 by using the vibration signals from force sensors, thus making a favorable tradeoff between computational efficiency and classification accuracy.

## II. PROPOSED APPROACH

### A. Experiment Setting

The proposed intelligent robot system is depicted in Fig. 1 and perceives the vibrational forces corresponding to the five common surface types in households (Fig. 2).

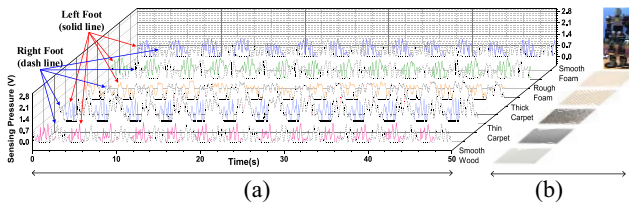


Fig. 2. (a) Raw force sensory data collected by our proposed system and (b) their corresponding five investigated indoor terrains.

- 1) A: Smooth and rigid wood flooring (smooth wood).
- 2) B: 0.3 cm thin soft carpet (thin carpet).
- 3) C: 0.6 cm thick rough carpet (thick carpet).
- 4) D: 0.9 cm thick foam with a rough surface (rough foam).
- 5) E: 0.9 cm thick foam with a smooth surface (smooth foam).

A KHR-3HV biped robot [9], equipped with 17 servomotors and an embedded controller, is employed to maintain stability during regular bipedal walking. A membrane force sensor [10] with sufficiently short response time ( $<1$  ms) and a large active area ( $39.6 \text{ mm} \times 39.6 \text{ mm}$ ) is attached beneath each robot foot. The output vibrational force, affected by the inertia and gravity during robot locomotion, is converted to a voltage output by a standard setup according to the sensor specification sheet. Then, the time-series samples of the foot-ground-contact force can be collected in the form of discrete voltage values by an A/D converter at a fixed sampling rate of  $T_s = 50 \text{ ms/point}$ . Therefore, a desired walking speed includes a sequence of  $M$  voltage points during a walking stride for a given biped robotic walking manner. We investigate the variation of foot-ground-contact forces at two prespecified walking speeds.

- 1) *Fast Speed*:  $M_F = 64$  points/stride.
- 2) *Slow Speed*:  $M_S = 88$  points/stride.

To build the intelligent surface-identification system on a microcomputer in a cost-efficient strategy for edge-computing applications, the low-cost Arduino with the 8-bit programmable CMOS microprocessor ATmega328 or the Jetson Nano combined with an embedded GPU are great options to deploy the feature extractor and the linear multiclass SVM classifier with low consumption of power and hardware resources.

The continuous and vibrational forces, detected by the force sensors, are transformed to digital voltage data with 10-bit resolution and then applied for time-domain feature extraction and dynamic surface classification on the microprocessor in real time. As the pattern recognition engine, the microprocessor outputs the predicted class for the current underlying surface and transmits the class to the robot system via the translation circuit (TC) as illustrated in Fig. 1.

### B. Pattern Recognition Engine

As a computing-efficient solution for online surface identification by the biped robot, a pattern-recognition engine that requires fewer hardware resources by combining an appropriate feature space with a high-efficiency classifier, has been well confirmed in this work.

1) *Time-Domain Feature Extraction*: As a crucial part of surface identification, feature extraction aims to facilitate the classification process by eliminating redundant data and noise from the raw sensory data. The time-domain features allow easier and quicker calculation, since no domain transformation

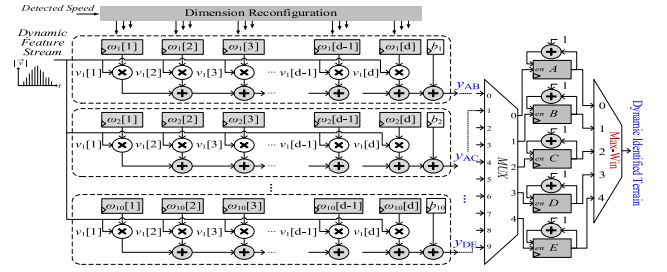


Fig. 3. Architecture of the online multiclass SVM classifier deployed on the programmable microprocessor.

is needed, and are thus more popular in pattern recognition. We have evaluated four time-domain features [11], i.e., root mean square (RMS), mean absolute value (MAV), variance (VAR), and waveform length (WL), which are extracted from the raw sensor-data stream inside a sliding window [16]. The window size indicates the number of sequential voltage points, used in the preprocessing stage to calculate each of the feature points for the above four time-domain features. An overlapped-window strategy, which slides the window by one voltage point at a time, is applied to calculate  $M$ -dimensional feature vectors of the above four features in case of a  $M$ -point vibration period at a designated walking speed. These  $M$ -dimensional feature vectors are described as

$$\vec{v}(n) = \{v(n), v(n+1), v(n+2), \dots, v(n+M-1)\} \quad (1)$$

where  $v(n)$  is a feature point calculated from a half-stride window of voltage points with one of the above four features. Compared to the raw sensor data, features can alleviate the signal vibration and achieve more robust classification results.

2) *Pattern Recognition Model*: For the resource-limited edge-computing platforms, the SVM classifier is still highly competitive with the ANN-based solutions due to its high computational efficiency with much fewer hardware-resource requirements, while achieving comparative classification accuracy. Since the original SVM is normally applicable only to binary classification problems, meta-strategies are required for solving the multiclass identification problem for  $m = 5$  different indoor ground surfaces.

As illustrated in Fig. 3, we employ a max-win strategy to solve the  $m$ -class classification problem by building  $m(m-1)/2$  binary SVM classifiers for each pair  $(i, j)$  of combined surfaces according to

$$f_k \left( \vec{\omega}_{ij}^T \cdot \vec{v}(k) + b_{ij} \right) \geq 1 - \xi_{ij}(k), \xi_{ij}(k) \geq 0 \quad (2)$$

where  $f_k(x)$  is a vector combing the identified labels of the  $k$ th surface type by each classifier in the set of  $m(m-1)/2$  binary SVM classifiers,  $\omega_{i,j}$  is a column vector referring to an  $M$ -dimensional weight vector trained by an off-line SVM classifier,  $b_{ij}$  is a scalar bias of the binary SVM classifier for each surface pair  $(i, j)$ , and  $\xi_{ij}(k)$  is a slack variable for reducing the training errors. Basically, the max-win-based multiclass solution predicts the class of the input testing terrain by using a voting strategy, which chooses the class with the highest vote number from all binary classifiers.

### C. Translation Circuit

We developed a TC, as shown in the middle part of Fig. 1, to connect the implemented pattern-recognition engine for the

online surface identification system to the controller embedded in the robot. Specifically, the TC consists of a sequentially connected demultiplexer, a D/A converter, an RC-coupled amplifier, and a multiplexer. The demultiplexer is used for transferring the identified surface label to the D/A converter via an appropriate route, while the multiplexer is used to select the correct feedback signal for the robot controller. We apply an RC-coupled amplifier to amplify the weak analog signal which identifies the predicted surface class, and then send it to the robot controller for feedback control of the robotic walking speed. Thus, the main purpose of the TC is to transform the signal and further expand the amplitude difference of the label signal for each surface, so that these signals are easier to be discriminated for speed adjustment of the robot.

#### D. Identification Result-Oriented Speed Configuration

To achieve a steady walk on various indoor ground-surface types, the robot system controls the walking speed by adjusting the configuration parameters of the servomotors, according to the  $f_s$  output of the TC, as illustrated in Fig. 1. The desired robot motions can be designed and modified by the robot controller from a computer in advance. To adaptively configure an appropriate walking speed for the biped robot according to the identified surface type, the dynamically predicted results from the pattern-recognition engine, used as the trigger signals for speed adjustment, should be transmitted to the robot controller. Thus, signal detector and value comparator are combined in the robot controller for selecting an appropriate walking speed matched with  $f_s$ . We can change the walking speed by modifying the number of robot-motor frames (i.e., frame rate  $f_r$ ) for each combined servomotor posture. Specifically,  $f_r$  results in 160 or 220 frames/stride in the case of the aforementioned two walking speeds, i.e.,  $M = 64$  or 88 points/stride.

### III. EXPERIMENT AND ANALYSIS

#### A. Dataset and Cross-Validation

To estimate the accuracy performance of our SVM pattern recognition model for multiple surface identification while the biped robot walks at two different speeds, 250 samples of the sensor data are separately collected for each surface type at each walking speed for tenfold cross-validation (CV). In each CV fold, 9/10 of the surface samples are used for off-line SVM training, employing the linear kernel and the hyperparameter  $C = 0.01$ , while 1/10 of the samples of each surface are used for model testing. Tenfold CV applies 10 validation iterations by alternating training and testing samples and is performed for each walking speed to obtain a robustness estimation. Precision, recall rate, and accuracy are employed as the main quality-evaluation metrics of the classification results.

#### B. Binary Classification at Variable Speed

The raw binary-classification performances for the ten possible pairs of the five surface types are investigated at the two different walking speeds (64 and 88 p/s). We explored the speed-change effect on the precision-recall curves (PRCs), which provide insights into the tradeoff between precision and recall, for setting the surface-classification threshold. All four feature types were evaluated and experimental results for RMS are illustrated Fig. 4. Most surface pairs can achieve maximal precision up to 100% for both speeds at reduced recall rates. This result indicates the SVM model achieves a low rate of

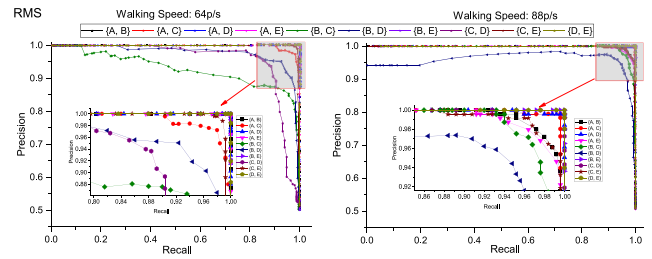


Fig. 4. PRCs for binary classification with the ten possible surface pairs of the five investigated surfaces, using the RMS feature at two different walking speeds (64 and 88 points/stride), respectively.

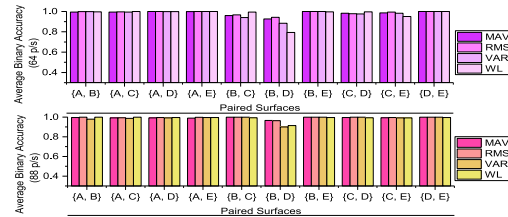


Fig. 5. Average accuracies of the tenfold cross validation with the ten binary SVM classifiers, corresponding to all possible pairs of the five investigated surfaces. The shown data is for the four features and the two different walking speeds.

false positive predictions, but fails to capture a significant portion of actual positive instances. Similar force waveforms from two surfaces (e.g., B and D) are likely leading to misidentification as each other. The maximal average precision (AP) reaches 99.6% for the two surface pairs {B, E} and {D, E} with RMS at 64 p/s. The mean AP (mAP) reaches  $> 91\%$  under different conditions at both walking speeds. In addition, we estimated the average accuracy (AA) of binary classification for each surface pair by changing the walking speed. Most surface pairs in different experimental settings achieve very high AA up to 100%, except for some cases, such as surface pair {B, D} at the speed of 88 p/s as shown in Fig. 5. Similar waveform characteristics of the sensing force due to a similar surface-texture roughness may bring the distinguishing difficulties between these two surfaces.

#### C. Multiobject Classification at Variable Speed

Due to the low computing complexity and high classification performance of the binary SVM classifier, we employ the “max-wins” voting strategy by combining multiple parallel binary SVMs for multiobject classification. The recall rate for a given surface in multiobject classification uses a one-versus-all scheme and the average recall rates are summarized in Fig. 6. Additionally, the tenfold APs of the multiobject SVM classification at the two speeds are determined and the experimental results are listed in Table I. Obviously, the RMS outperforms the other three features concerning recall rate and mAP at both investigated walking speeds of the biped robot. The friction parameters of the surfaces are capable to generate differentiable classification data even for the same stiffness while the robot walks at different speeds. The nonproportional response concerning the walking speeds asks for setting an appropriate speed for each given surface type.

Additionally, the proposed online surface-identification system is sensitive enough to adjust the walking speed in time according to the predicted result for the underlying surface. As

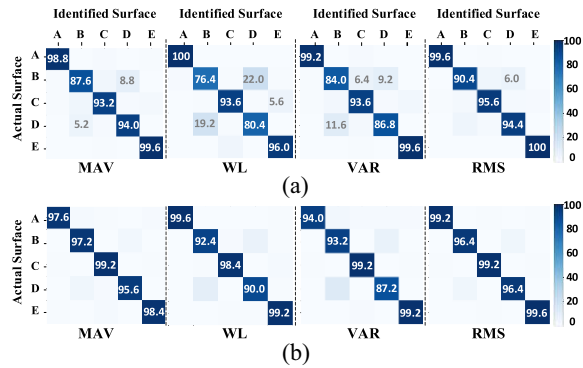


Fig. 6. Confusion matrices of the average recall rates (%), employing the tenfold CV multiobject SVM recognition for five different surfaces using four different features at two walking speeds, respectively. (a) 64 point/stride. (b) 88 point/stride.

TABLE I  
TENFOLD AP OF MULTIOBJECT SVM CLASSIFICATION

Walking Speed	Feature Vector	Average Precision (%) of each surface using multi-object SVM classification in 10 folds					mAP (%)
		Smooth Wood	Thin Carpet	Thick Carpet	Rough Foam	Smooth Foam	
64 p/s	MAV	99.19	90.87	94.72	90.73	97.65	94.63
	WL	99.21	79.58	95.12	78.21	94.12	89.25
	RMS	99.60	93.39	94.84	92.91	99.21	<b>95.99</b>
	VAR	99.20	85.71	91.05	89.67	97.27	92.58
88 p/s	MAV	99.19	95.29	97.64	97.15	98.79	97.61
	WL	<b>100</b>	90.23	98.79	92.98	97.64	95.93
	RMS	99.60	96.40	99.20	96.40	99.20	<b>98.16</b>
	VAR	99.58	85.66	98.02	91.60	98.80	94.73

TABLE II  
WALKING SPEED ADJUSTMENT AND LATENCY

Walking Speed (points/stride)	T (s)	Frame rate $f_f$ (frames/stride)	Speed Adjustment Latency (s)
$M_F=64$	3.2	160	$\sim 3.0$ (160 $\rightarrow$ others)
$M_S=88$	4.4	220	$\sim 5.3$ (220 $\rightarrow$ others)

\*T=vibration period;  $f_f$  indicates frame rate of robot stride.

TABLE III  
COMPARISON WITH OTHER STATE-OF-THE-ART WORKS

Method	Sensor	Feature Extraction	Classifier	Accuracy (%)
[2]	Capacitive Tactile & IMU	Peak Amplitude of Sum, etc.	SVMs	82.5
[13]	Vision & Accelerometer	DFT, etc.	FT-S2ELM	$\sim 90.2$
[14]	Vision & Acoustics	Triplet Loss & MobileNet	AdapNet++	73.21 (mR) 94.8 (clustering)
[15]	Audio & Vision	Audio: VAE Vision: CNN	CNN	80
[16]	Force	Combined MAV, RMS, VAR, WL	SVMs	93.7 (mA)
This work	Force	RMS	SVMs	$M_F \rightarrow 92.6$ (mA) $M_S \rightarrow 94.6$ (mA)

summarized in Table II, the two investigated walking speeds take  $T = 3.2$  and  $4.4$  s per stride, respectively. The proposed solution’s processing speed on the ATmega328 microprocessor is sufficient for real-time operation, since the overall processing time of the online multiobject SVM system consumes only about 0.8 ms per stride. Thus, we could preset the suitable speed easily for each surface and adjust the speed immediately according to the identification-result feedback of the

underlying surface. A performance comparison with important existing solutions [2], [13], [14], [15], [16] is provided in Table III.

#### IV. CONCLUSION

In this work, we propose an accurate and fast surface-identification system based on a single sensing modality by force sensors and verified this system at two different walking speeds. Four time-domain features are evaluated and the RMS feature turns out to be most suitable for surface classification. The walking speed seems to be not a strictly limiting factor for the classification performance. Nevertheless, the slower walking velocity at 88 p/s does attain the highest performance in terms of mAP in multiobject classification. The proposed efficient computing scheme has sufficiently high accuracy and can thus lead to extensive applications in mobile robots and edge devices.

#### REFERENCES

- [1] K. Otsu, M. Ono, T. J. Fuchs, I. Baldwin, and T. Kubota, “Autonomous terrain classification with co- and self-training approach,” *IEEE Rob. Autom. Lett.*, vol. 1, no. 2, pp. 814–819, Jul. 2016.
- [2] X. A. Wu, T. M. Huh, A. Sabin, S. A. Suresh, and M. R. Cutkosky, “Tactile sensing and terrain-based gait control for small legged robots,” *IEEE Trans. Rob.*, vol. 36, no. 1, pp. 15–27, Feb. 2020.
- [3] A. Ahmadi, T. Nygaard, N. Kottege, D. Howard, and N. Hudson, “Semi-supervised gated recurrent neural networks for robotic terrain classification,” *IEEE Rob. Autom. Lett.*, vol. 6, no. 2, pp. 1848–1855, Apr. 2021.
- [4] R. Matsumura, M. Shiomi, T. Miyashita, H. Ishiguro, and N. Hagita, “What kind of floor am I standing on? Floor surface identification by a small humanoid robot through full-body motions,” *Adv. Robot.*, vol. 29, no. 7, pp. 469–480, 2015.
- [5] X. Guo et al., “Soft foot sensor design and terrain classification for dynamic legged locomotion,” in *Proc. 3rd IEEE Int. Conf. Soft Rob.*, May 2020, pp. 550–557.
- [6] Z. Awad, R. Akel, N. Maalouf, and I. H. Elhadj, “Terrain classification for bipedal robots: A comparative study,” in *Proc. 10th Inst. Electri. Electron. Eng. Int. Conf. Cyber Technol. Autom. Con. Intell. Syst.*, 2020, pp. 61–66.
- [7] S. Bhattacharya et al., “Surface-property recognition with force sensors for stable walking of humanoid robot,” *IEEE Access*, vol. 7, pp. 146443–146456, 2019.
- [8] S. Ryu and S.-C. Kim, “Embedded identification of surface based on multirate sensor fusion with deep neural network,” *IEEE Embed. Syst. Lett.*, vol. 13, no. 2, pp. 49–52, Jun. 2021.
- [9] *KHR-3HV Robot*. Kondo Kagaku Co., Ltd., Japan. Accessed: Dec. 20, 2022. [Online]. Available: <https://kondo-robot.com/product/03110e>
- [10] *Specification of Membrane Force Sensors Provided by Alpha*. Taiwan Alpha Electronic Co., Taiwan. Accessed: Apr. 10, 2022. [Online]. Available: <http://www.taiwanalpha.com/en/products/21>
- [11] A. Phinyomark, C. Limsakul, and P. Phukpattaranont, “A novel feature extraction for robust EMG pattern recognition,” *J. Comput.*, vol. 1, no. 1, pp. 71–80, 2009.
- [12] A. Milella, G. Reina, and J. Underwood, “A self-learning framework for statistical ground classification using radar and monocular vision,” *J. Field Robot.*, vol. 32, no. 1, pp. 20–41, 2015.
- [13] W. Lv, Y. Kang, W. X. Zheng, Y. Wu, and Z. Li, “Feature-temporal semi-supervised extreme learning machine for robotic terrain classification,” *IEEE Trans. Circuits Syst. II, Exp. Briefs*, vol. 67, no. 12, pp. 3567–3571, Dec. 2020.
- [14] J. Zörn, W. Burgard, and A. Valada, “Self-supervised visual terrain classification from unsupervised acoustic feature learning,” *IEEE Trans. Robot.*, vol. 37, no. 2, pp. 466–481, Apr. 2021.
- [15] A. Kurobe, Y. Nakajima, K. Kitani, and H. Saito, “Audio-visual self-supervised terrain type recognition for ground mobile platforms,” *IEEE Access*, vol. 9, pp. 29970–29979, 2021.
- [16] A. Luo et al., “Surface recognition via force-sensory walking-pattern classification for biped robot,” *IEEE Sensors J.*, vol. 21, no. 8, pp. 10061–10072, Apr. 2021.